Biochemical and Biophysical Research Communications 435 (2013) 250–254

Contents lists available at SciVerse ScienceDirect

Biochemical and Biophysical Research Communications

journal homepage: www.elsevier.com/locate/ybbrc

Localization of the regulatory particle subunit Sem1 in the 26S proteasome

Stefan Bohn [1], Eri Sakata [2], Florian Beck, Ganesh R. Pathare, Jérôme Schnitger, Istvan Nágy, Wolfgang Baumeister *, Friedrich Förster *

Max-Planck Institute of Biochemistry, Department of Molecular Structural Biology, D-82152 Martinsried, Germany

ARTICLE INFO

Article history:
Received 17 April 2013
Available online 1 May 2013

Keywords:
26S proteasome
Sem1
Proteasome-COP9-initiation factor domain
TREX-2
Cryo-electron microscopy

ABSTRACT

The ubiquitin–proteasome system is responsible for regulated protein degradation in the cell with the 26S proteasome acting as its executive arm. The molecular architecture of this 2.5 MDa complex has been established recently, with the notable exception of the small acidic subunit Sem1. Here, we localize the C-terminal helix of Sem1 binding to the PCI domain of the subunit Rpn7 using cryo-electron microscopy single particle reconstruction of proteasomes purified from yeast cells with *sem1* deletion. The approximate position of the N-terminal region of Sem1 bridging the cleft between Rpn7 and Rpn3 was inferred based on site-specific cross-linking data of the 26S proteasome. Our structural studies indicate that Sem1 can assume different conformations in different contexts, which supports the idea that Sem1 functions as a molecular glue stabilizing the Rpn3/Rpn7 heterodimer.

1. Introduction

The 26S proteasome is a cytosolic self-compartmentalizing protease capable of degrading proteins that are either defective or no longer needed by the cell [1]. Most proteasomal substrates to be degraded are marked for degradation by the covalent fusion of polyubiquitin, which confers selectivity to the 26S proteasome [2]. The 26S proteasome consists of the 20S core particle (CP), which is also found in archaea and some bacteria, and the eukaryote-specific 19S regulatory particle (RP), which caps one or both ends of the cylinder-shaped CP. The CP hosts the proteolytically active sites whereas the RP is responsible for substrate binding, unfolding of the substrate and its translocation into the CP, but also for removing the polyubiquitin chain.

The high-resolution structure of the CP has been determined almost two decades ago [3,4] but only recently the architecture of the RP has been revealed by cryo-electron microscopy (EM) [5–7]. Using different approaches atomic models of all canonical RP subunits have been located unambiguously in cryo-EM maps with the notable exception of one subunit, namely the 89-residue acidic subunit Sem1 [7].

Sem1 was identified as a subunit of the lid subcomplex of the RP [8,9]. Like the other proteasome subunits, Sem1 is conserved throughout eukaryotes and its ortholog in mammals is DSS1 (Deleted-in-Split-Hand/Split-Foot-1). Due to its relatively small size it has been difficult to determine its stoichiometry, but different biochemical experiments suggested that Sem1 is a stoichiometric component [8,10]. Cross-linking analysis and identifications of assembly intermediates indicated that Sem1 may form a sub-complex with the proteasome subunits Rpn3 and Rpn7 [11–13]. However, the precise interaction sites could not be mapped so far. Sem1 has been shown to mediate the association of proteasomes with sites of DNA double strand breaks [14], but the precise function of Sem1 in the 26S proteasome remained enigmatic.

Sem1 is also a component of at least three other complexes: the E3 ligase complex BRCC [15], the TREX-2 transcription-export complex [16,17], and the Thp3–Csn12 complex involved in transcription elongation [17,18]. Whether this promiscuity of Sem1 reflects a functional interplay among the involved complexes or hints at a general structural role of Sem1 in stabilizing these complexes is unclear. In yeast Sem1 deletion is not lethal albeit the strains are temperature-sensitive [15], whereas DSS1 is essential in the embryonic development of higher eukaryotes [19].

Sem1/DSS1 has been co-crystallized in two complexes. When bound to BRCA2, a subunit of BRCC complex, DSS1 exhibits only short secondary structure elements and it wraps around BRCA2 [20]. In the TREX-2 transcription-export complex, the C-terminal 19 residues of Sem1 form an α-helix, which binds to Thp1, whereas the remaining N-terminal region, which wraps mostly around Thp1, is essentially devoid of secondary structure elements [21].

Abbreviations: PCI, proteasome-COP9-initiation factor; CP, core particle; RP, regulatory particle; XL/MS, cross-linking/mass-spectrometry.

* Corresponding authors. Fax: +49 89 8578 2641.
E-mail addresses: baumeist@bichem.mpg.de (W. Baumeister), foerster@bichem.mpg.de (F. Förster).
[1] Current address: Department of Cellular and Molecular Pharmacology, University of California, San Francisco, CA, USA.
[2] Current address: Department of Molecular Biophysics and Biochemistry, Yale University, School of Medicine, New Haven, CT, USA.

0006-291X/$ - see front matter © 2013 Elsevier Inc. All rights reserved.
http://dx.doi.org/10.1016/j.bbrc.2013.04.069

Structural studies of Sem1 suggested that its interaction partner co-determines its structure. The architecture of Thp1 is common with that of Rpn3 and Rpn7, N-terminal tetratricopeptide-like repeats (TPRs) followed by a proteasome-COP9-inititiation factor (PCI) domain. This has led to the proposal that Sem1 binds similarly in the 26S proteasome as observed in the TREX-2 complex [21].

In this study, we localize Sem1 in the RP by comparison of cryo-EM maps of wild-type *Saccharomyces cerevisiae* 26S proteasomes with holocomplexes from *sem1* deletion (*sem1Δ*) strains. The results are consistent with data from chemical cross-linking in conjunction with mass-spectrometry (XL-MS), which specify the location of the Sem1 C-terminus. Our results show that Sem1 binds to the proteasomal PCI subunits in a different manner from that observed in the TREX-2 complex and support the idea that the primary role of Sem1 is a stabilization of the Rpn3/Rpn7 heterodimer.

2. Materials and methods

2.1. Purification, knock-out and reconstituted complex

For cryo-EM reconstruction, intact 26S proteasomes from wild-type and Sem1 deletion strain were purified via RPN11-3×FLAG tag (yeast background W303), as described previously [22]. The eluate was further enriched [23] and analyzed by MS. The enriched fraction of the double-capped 26S proteasomes was used for further analysis. For co-expression, 8×His-Rpn7 and TEV-cleavable GST-Sem1 from *Drosophila melanogaster* were expressed in *Escherichia coli* BL21-codon plus (DE3) RP cells. The Rpn7-Sem1 complex was purified by subsequent NiNTA (50 mM Tris pH 8.0, 150 mM NaCl, 20 to 250 mM imidazole) and GST-tag pulldown with (20 mM Tris pH 7.5, 150 mM NaCl). The GST tag was removed from Sem1 by TEV cleavage.

2.2. Cryo-EM

26S proteasomes were applied to holey carbon grids (Quantifoil Micro Tools, Germany), vitrified and imaged using a Titan Krios microscope at 200 kV (final magnification: 150 k; object pixel size: 1 Å) in an automated manner using TOM^2 [24]. The contrast transfer function was determined and micrographs were deconvoluted by phase-flipping in TOM [25]. From 6619 micrographs, 215,480 particles were selected based on [26], and 3D reconstruction was performed using XMIPP [27].

3. Results

3.1. A rod-like density near the helices of the Rpn7 winged helix motif is unassigned in the wt map

It has been shown previously that the PCI subunits assemble into a horseshoe-shaped module with the subunit order Rpn9, Rpn5, Rpn6, Rpn7, Rpn3, and Rpn12 [5,6,28]. The PCI domains form the inter-subunit contacts in the horseshoe module. The atomic models of the Rpn7 and Rpn3 PCI domains explain the electron density of the wildtype 26S proteasome in the corresponding area with the exception of a rod-like density at the Rpn7 flank that faces the neighboring PCI subunit Rpn3 and some density stretch connecting Rpn3 and Rpn7 (Fig. 1). More precisely, the unassigned rod-like density is positioned near the three helices of the winged helix motif of Rpn7 [29]. This rod-like density is approximately 1 nm in diameter and 3 nm in length, which corresponds to an α-helix of approximately 20 amino acid residues.

3.2. Sem1 is closely associated to PCI subunit of Rpn7

Biochemical data suggest that Sem1 forms a sub-complex with Rpn3 and Rpn7 [11,12]. Thus, we hypothesized that the unassigned density at the Rpn7 flank may correspond to a segment of Sem1. In the crystal structure of the TREX-2 complex Sem1 has a 19-residue helix at its C-terminus, which would be a plausible candidate for the rod-like density.

To characterize the binding of Sem1 structurally, we purified 26S proteasomes from a strain lacking the gene *sem1* for subsequent single particle cryo-EM analysis. MS analysis of the purified *sem1Δ*-26S proteasome showed that all canonical proteasomal subunits except for Sem1 are present in approximately equal amounts (Fig. S1). Compared to wt-26S preparations comparable

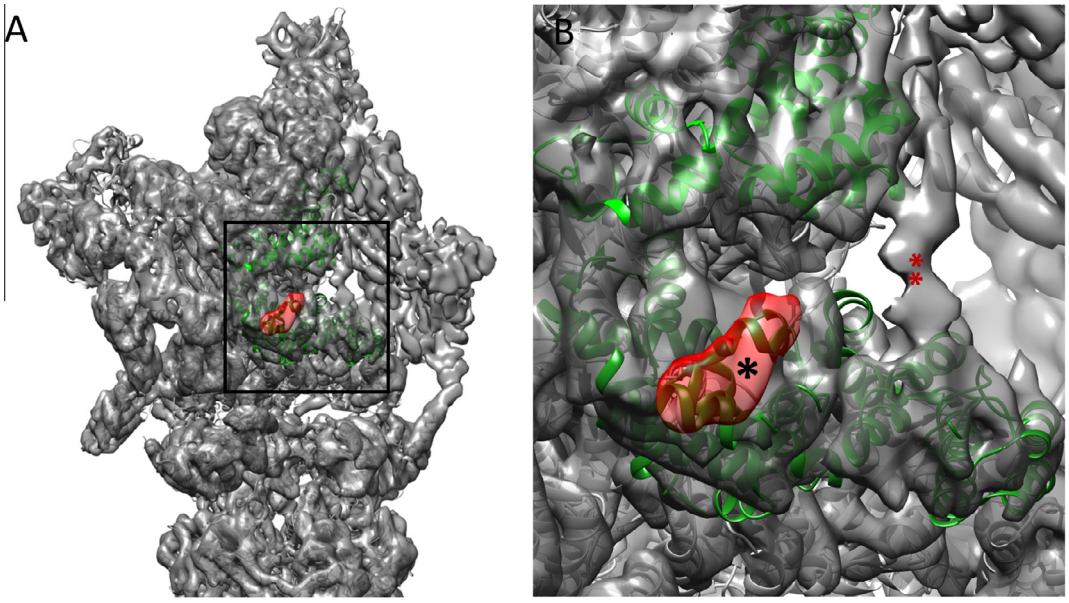

Fig. 1. Current structure and atomic model of the 26S proteasome from *S. cerevisiae*. (A) Cryo-EM density of the asymmetric unit of the wildtype 26S proteasome (gray, EMDB 2135). The atomic model (PDB code: 4b4t) is shown in black, with Rpn3 in light green and Rpn7 in dark green. (B) Enlarged view of Rpn3 and Rpn7. In close proximity to the C-terminal PCI domain of Rpn7, unassigned densities (* and **), one of which rod-shaped resembling an α-helix (*), can be observed. These densities cannot be attributed to either Rpn7 or Rpn3.

amounts of intact 26S holocomplexes were present in the *sem1Δ*-26S preparations used for EM (Fig. S1). The single particle reconstruction of the *sem1Δ*-26S proteasomes exhibited a resolution of 10.4 Å (Fourier Shell Correlation, FSC = 0.5) or 8.3 Å for FSC = 0.3 (Fig. 2, S2). The density of the *sem1Δ*-26S proteasome is significantly different from that of the wt-26S proteasome indicating that Sem1 is indeed a stoichiometric component of the 26S proteasome. Comparison of the *sem1Δ*-26S map to the density of the wt-26S proteasome [7] filtered to the same resolution by means of a difference map reveals that the rod-like density adjacent to the Rpn7 PCI domain is not present in the *sem1Δ* density. Considering that the N-terminal region of Sem1 does not exhibit a defined tertiary structure in any crystal structures [20,21], we assigned the rod-like density as the C-terminal helix of Sem1.

Assembly studies of the proteasome suggested that the interaction of Sem1 with Rpn7 is stronger than that with Rpn3 [13]. It was suggested that these two subunits might form a stable heterodimer. To verify the physical interaction of Rpn7 with Sem1, we co-expressed Rpn7 and GST-Sem1 in *E. coli* cells. Indeed, Rpn7 co-purifies with Sem1 (Fig. S3), indicating the tight interaction between these two proteins. In addition to this most pronounced difference upon Sem1 removal we also observed more subtle structural differences in the regions corresponding to Rpn7 and Rpn3 suggesting that Sem1 impacts the structure of these subunits as well.

3.3. Model of Sem1 in the 26S holocomplex

To localize the N-terminal parts of Sem1 approximately and to determine the directionality of the C-terminal helix in its corresponding density we built a model of Sem1 in the context of the current structural model of the wt-26S proteasome [7] as well as existing chemical cross-linking and mass-spectrometry (XL/MS) data [30]. These XL/MS data indicate lysine residue-pairs with a distance of less than approximately 25–30 Å [31].

Out of the nine Sem1 lysine residues, K18, K20 and K26 cross-link to lysines of the RP subunits Rpn3 and Rpn7 (Fig. S4). These cross-links suggest that the Sem1 N-terminus is positioned in proximity to the N-terminal domain of Rpn3 and the C-terminus of Rpn7. Both regions were not modeled in the high-resolution structure of the 26S proteasome [7], but their approximate locations can be inferred. The C-terminus of Rpn7 is located in a helical bundle that tethers the lid together (Fig. 3). The resolution of the N-terminal domain of Rpn3 containing TPRs is not sufficient to allow tracing the helix topology (Fig. 3). However, both density segments, helical bundle and Rpn3 N-terminus, are adjacent to each other, which indicates that the cross-links are consistent. Thus, the N-terminal segment of Sem1, which is devoid of any secondary structure in the available X-ray structures, is likely to be localized in a cleft between the PCI domains of Rpn7 and Rpn3. It contacts the helical bundle of the lid and the N-terminal domain of Rpn3. The C-terminus of the C-terminal helix of Sem1 likely projects outward, which results in a shorter path of the peptide towards its N-terminus.

4. Discussion

4.1. Sem1 tethers Rpn7, Rpn3 and lid helical bundle

Our cryo-EM analysis of purified 26S proteasomes constitutively lacking Sem1 confirms that Sem1 is a stoichiometric component of the 26S proteasome. By comparing the cryo-EM single particle reconstruction of the *sem1Δ*-26S proteasome to that of the wt-26S proteasome we could identify the C-terminal helix of Sem1 binding to the winged helix of Rpn7. XL/MS data further reveal the approximate positions of the Sem1 N-terminal parts. Based on these data we could infer the direction of the Sem1 C-terminal helix and the approximate path of the Sem1 peptide.

The position of Sem1 in the cleft between the PCI domains of Rpn7 and Rpn3 is consistent with our current understanding of the assembly of the lid sub-complex [12], suggesting that Rpn3, Rpn7, and Sem1 form a stable lid precursor complex. Moreover, the positioning of N-terminus of Sem1 agrees with biochemical studies that identified a specific Rpn3/S3-interacting motif (R3IM) in this segment [32].

4.2. Sem1 binds PCI-domains in at least two distinct ways

In the two hitherto solved structures of Sem1-containing complexes, the TREX-2 transcription-export complex [21] and BRCC [15], Sem1 adopts entirely different conformations (Fig. 3). Thus, the structure of Sem1 seems to be co-determined by its interaction partners, Thp1 and BRCA2, respectively, which have different folds. Since Thp1 and Rpn7 are structurally similar it has been suggested

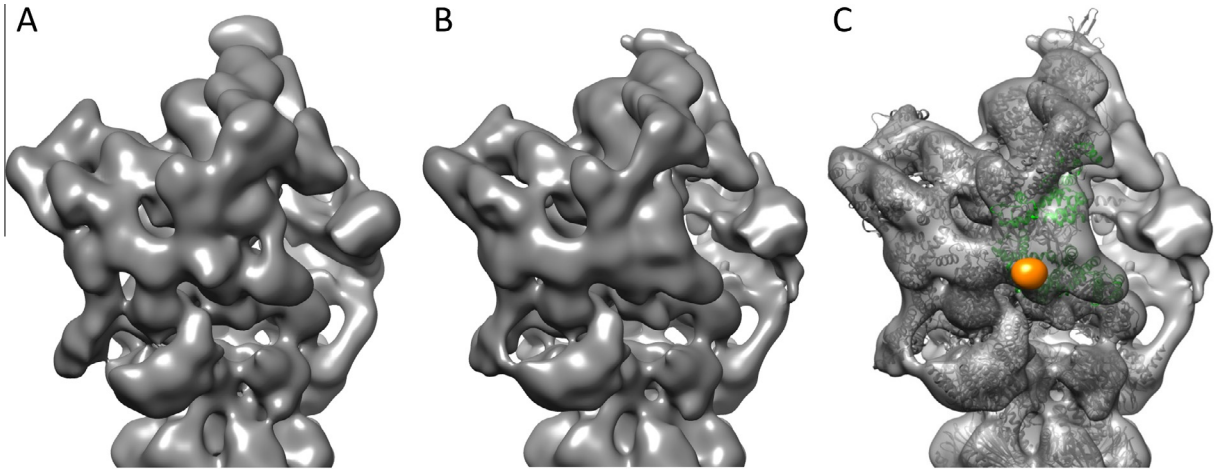

Fig. 2. Comparison of wild-type and *sem1Δ* 26S proteasomes. (A) The cryo-EM density of the wild-type 26S proteasome (EMDB 2135) filtered to 14 Å to focus on the main features of the structure. (B) Reconstruction of the *sem1Δ*-26S proteasome filtered to the same resolution. (C) Difference map superpositioned on the *sem1Δ*-26S proteasome structure. The most significant difference between wild-type and *sem1Δ* densities (orange) co-localizes with the unassigned helical density (Fig. 1B). The atomic models of Rpn7, Rpn3 and the remaining proteasomal subunits are shown in dark green, light green and black, respectively.

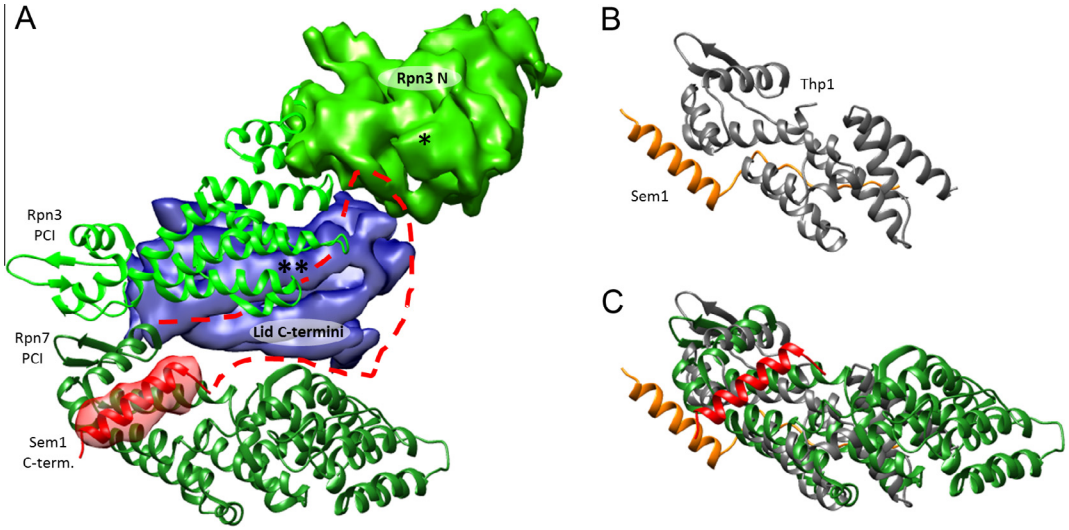

Fig. 3. Interactions of Sem1 with RP proteins. (A) The location of the N-terminal unstructured region of Sem1 (orange dotted line) can be estimated based on the approximated location of Rpn3:K58 (*, cross-linking to Sem1:26) and Rpn7:K413 (**, cross-linking to Sem1:18 and Sem1:20), respectively (Rpn3, light green, and Rpn7, dark green, from PDB entry 4b4t). In the wildtype 26S proteasome the N-terminal domain of Rpn3 (Rpn3N) can be mapped to the density depicted in green. The Rpn7 C-terminus is located in a large helical bundle comprising the C-termini of the lid subunits (**, blue). (B) Sem1 binds to the Thp1–Sac3 heterodimer via the C-terminal Winged Helix domain of Thp1 (Sem1 in red, Thp1 in gray; PDB code: 3T5V). (C) The C-terminal PCI folds of Thp1 (gray) and Rpn7 (green) were structurally aligned using MUSTANG [34]. The position of the C-terminal helix of Sem1 (red) in the Thp1-Sem1 complex differs significantly from the position at Rpn7 in the context of the 26S proteasome (orange).

that Sem1 binds to Rpn7 in a mode similar to the one observed for Thp1 [21]. In the TREX-2 structure Sem1's C-terminal α-helix was found to bind the PCI-domain of Thp1 (Fig. 3B), whereas its remaining N-terminal region, which is essentially devoid of secondary structure elements, wraps around Thp1.

The binding modes of Sem1 to the PCI-domains of Rpn7 and Thp1 can be compared after structural alignment of both PCI domains (Fig. 3C). This structural comparison reveals that the binding modes of Sem1 to the two PCI domains are entirely different. If the C-terminal helix of Sem1 would bind to Rpn7 in a similar mode as to Thp1, it would be positioned in a cleft between Rpn6 and Rpn7 in the context of the 26S holocomplex (Fig. 4). Surprisingly, our cryo-EM data of the *sem1Δ* 26S proteasome shows that this helix binds to the opposite flank of Rpn7 and also the localization of the Sem1 C-terminus is not compatible with the binding mode observed in the TREX-2 complex. Thus, Sem1 appears to bind to two structurally similar proteins in different modes.

4.3. Functional implications of the Sem1 position

The flexibility appears to be well-suited for a protein to serve as a 'molecular glue' [33]. The position of Sem1 in the cleft between the PCI domains of Rpn3 and Rpn7 seems well suited to tether these two subunits together. Moreover, the notable structural rearrangement of Rpn3 and Rpn7 upon Sem1 deletion also supports the notion of Sem1 stabilizing the Rpn3–Rpn7 subcomplex albeit the number of intact 26S proteasomes is only moderately decreased in *sem1Δ*-26S proteasome preparations (Fig. S1B). However, the startling question is why a single protein is used for stabilization of at least four different complexes (Rpn3/Rpn7, TREX-2, BRCC, and Thp3–Csn12 complex). It is conceivable that the stabilization of these complexes by Sem1 is a means of regulating functionally linked complexes. Intriguingly, all of these four complexes are involved in the UPP.

Furthermore, it is interesting that Sem1 binds to the flank of Rpn7's winged helix motif where nucleotides bind in many other structurally related proteins [29]. To date there is no experimental evidence for direct binding of the proteasomal PCI domains to DNA or RNA, but it has been shown that the 26S proteasome gets recruited to sites of double strand breaks (DSBs) [14]. Intriguingly, Sem1 is essential for this DSB recruitment, but undoubtedly further

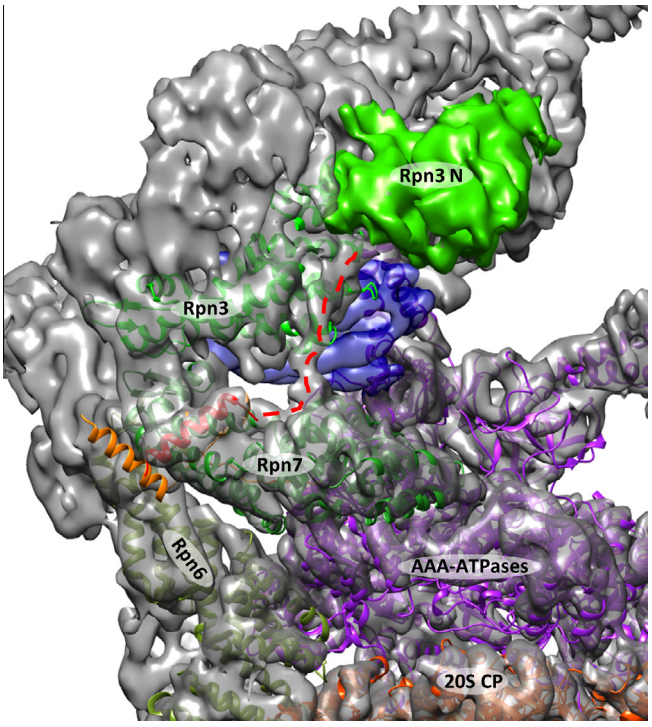

Fig. 4. Model of Sem1 in the 26S proteasome. Sem1, in the context of the 26S proteasome (orange), binds a different PCI interface than in the Thp1-Sac3 complex, which would place Sem1 (red) in a cleft between Rpn6 (olive green) and Rpn7 (dark green). Unassigned density from the wt-26S proteasome model (orange dotted line) suggests the N-terminal unstructured region of Sem1 binds the N-terminal portion of Rpn3 (Rpn3N, light green) before winding its way towards the coiled-coil bundle (blue) containing the C-terminal coiled-coil of Rpn7. AAA-ATPases in purple, 20S CP α-ring in red–orange.

structural–functional investigations are needed to elucidate the role of the 26S proteasome in DNA repair.

Acknowledgments

We thank Keiji Tanaka and Yasushi Saeki for providing the *sem1Δ* strain. Our research is supported by funding from European Union Seventh Framework Programme PROSPECTS (Proteomics Specification in Space and Time Grant HEALTH-F4-2008-201648), Deutsche Forschungsgemeinschaft (SFB-1035 to W.B.), and Human Frontiers Science Program (Career Development Award to F.F.).

Appendix A. Supplementary data

Supplementary data associated with this article can be found, in the online version, at http://dx.doi.org/10.1016/j.bbrc.2013.04.069.

References

[1] D. Voges, P. Zwickl, W. Baumeister, The 26S proteasome: a molecular machine designed for controlled proteolysis, Annu. Rev. Biochem. 68 (1999) 1015–1068.
[2] A. Hershko, A. Ciechanover, A. Varshavsky, Basic medical research award. The ubiquitin system, Nat. Med. 6 (2000) 1073–1081.
[3] J. Lowe, D. Stock, B. Jap, P. Zwickl, W. Baumeister, R. Huber, Crystal structure of the 20S proteasome from the archaeon T. acidophilum at 3.4 A resolution, Science 268 (1995) 533–539.
[4] M. Groll, L. Ditzel, J. Lowe, D. Stock, M. Bochtler, H.D. Bartunik, R. Huber, Structure of 20S proteasome from yeast at 2.4 A resolution, Nature 386 (1997) 463–471.
[5] G.C. Lander, E. Estrin, M.E. Matyskiela, C. Bashore, E. Nogales, A. Martin, Complete subunit architecture of the proteasome regulatory particle, Nature 482 (2012) 186–191.
[6] K. Lasker, F. Forster, S. Bohn, T. Walzthoeni, E. Villa, P. Unverdorben, F. Beck, R. Aebersold, A. Sali, W. Baumeister, Molecular architecture of the 26S proteasome holocomplex determined by an integrative approach, Proc. Natl. Acad. Sci. USA 109 (2012) 1380–1387.
[7] F. Beck, P. Unverdorben, S. Bohn, A. Schweitzer, G. Pfeifer, E. Sakata, S. Nickell, J.M. Plitzko, E. Villa, W. Baumeister, F. Forster, Near-atomic resolution structural model of the yeast 26S proteasome, Proc. Natl. Acad. Sci. USA 109 (2012) 14870–14875.
[8] T. Sone, Y. Saeki, A. Toh-e, H. Yokosawa, Sem1p is a novel subunit of the 26 S proteasome from Saccharomyces cerevisiae, J. Biol. Chem. 279 (2004) 28807–28816.
[9] M. Funakoshi, X. Li, I. Velichutina, M. Hochstrasser, H. Kobayashi, Sem1, the yeast ortholog of a human BRCA2-binding protein, is a component of the proteasome regulatory particle that enhances proteasome stability, J. Cell Sci. 117 (2004) 6447–6454.
[10] E. Sakata, F. Stengel, K. Fukunaga, M. Zhou, Y. Saeki, F. Forster, W. Baumeister, K. Tanaka, C.V. Robinson, The catalytic activity of ubp6 enhances maturation of the proteasomal regulatory particle, Mol. Cell 42 (2011) 637–649.
[11] M. Sharon, T. Taverner, X.I. Ambroggio, R.J. Deshaies, C.V. Robinson, Structural organization of the 19S proteasome lid: insights from MS of intact complexes, PLoS Biol. 4 (2006) e267.
[12] K. Fukunaga, T. Kudo, A. Toh-e, K. Tanaka, Y. Saeki, Dissection of the assembly pathway of the proteasome lid in *Saccharomyces cerevisiae*, Biochem. Biophys. Res. Commun. 396 (2010) 1048–1053.
[13] R.J. Tomko Jr., M. Hochstrasser, Incorporation of the Rpn12 subunit couples completion of proteasome regulatory particle lid assembly to lid-base joining, Mol. Cell 44 (2011) 907–917.
[14] N.J. Krogan, M.H. Lam, J. Fillingham, M.C. Keogh, M. Gebbia, J. Li, N. Datta, G. Cagney, S. Buratowski, A. Emili, J.F. Greenblatt, Proteasome involvement in the repair of DNA double-strand breaks, Mol. Cell 16 (2004) 1027–1034.
[15] N.J. Marston, W.J. Richards, D. Hughes, D. Bertwistle, C.J. Marshall, A. Ashworth, Interaction between the product of the breast cancer susceptibility gene BRCA2 and DSS1, a protein functionally conserved from yeast to mammals, Mol. Cell. Biol. 19 (1999) 4633–4642.
[16] M.B. Faza, S. Kemmler, S. Jimeno, C. Gonzalez-Aguilera, A. Aguilera, E. Hurt, V.G. Panse, Sem1 is a functional component of the nuclear pore complex-associated messenger RNA export machinery, J. Cell Biol. 184 (2009) 833–846.
[17] G.M. Wilmes, M. Bergkessel, S. Bandyopadhyay, M. Shales, H. Braberg, G. Cagney, S.R. Collins, G.B. Whitworth, T.L. Kress, J.S. Weissman, T. Ideker, C. Guthrie, N.J. Krogan, A genetic interaction map of RNA-processing factors reveals links between Sem1/Dss1-containing complexes and mRNA export and splicing, Mol. Cell 32 (2008) 735–746.
[18] S. Jimeno, C. Tous, M.L. Garcia-Rubio, M. Ranes, C. Gonzalez-Aguilera, A. Marin, A. Aguilera, New suppressors of THO mutations identify Thp3 (Ypr045c)–Csn12 as a protein complex involved in transcription elongation, Mol. Cell. Biol. 31 (2011) 674–685.
[19] M.A. Crackower, S.W. Scherer, J.M. Rommens, C.C. Hui, P. Poorkaj, S. Soder, J.M. Cobben, L. Hudgins, J.P. Evans, L.C. Tsui, Characterization of the split hand/split foot malformation locus SHFM1 at 7q21.3–q22.1 and analysis of a candidate gene for its expression during limb development, Hum. Mol. Genet. 5 (1996) 571–579.
[20] H. Yang, P.D. Jeffrey, J. Miller, E. Kinnucan, Y. Sun, N.H. Thoma, N. Zheng, P.L. Chen, W.H. Lee, N.P. Pavletich, BRCA2 function in DNA binding and recombination from a BRCA2–DSS1–ssDNA structure, Science 297 (2002) 1837–1848.
[21] A.M. Ellisdon, L. Dimitrova, E. Hurt, M. Stewart, Structural basis for the assembly and nucleic acid binding of the TREX-2 transcription-export complex, Nat. Struct. Mol. Biol. 19 (2012) 328–336.
[22] Y. Saeki, E.A. Toh, T. Kudo, H. Kawamura, K. Tanaka, Multiple proteasome-interacting proteins assist the assembly of the yeast 19S regulatory particle, Cell 137 (2009) 900–913.
[23] E. Sakata, S. Bohn, O. Mihalache, P. Kiss, F. Beck, I. Nagy, S. Nickell, K. Tanaka, Y. Saeki, F. Forster, W. Baumeister, Localization of the proteasomal ubiquitin receptors Rpn10 and Rpn13 by electron cryomicroscopy, Proc. Natl. Acad. Sci. USA 109 (2012) 1479–1484.
[24] A. Korinek, F. Beck, W. Baumeister, S. Nickell, J.M. Plitzko, Computer controlled cryo-electron microscopy–TOM(2) a software package for high-throughput applications, J. Struct. Biol. 175 (2011) 394–405.
[25] S. Nickell, F. Forster, A. Linaroudis, W.D. Net, F. Beck, R. Hegerl, W. Baumeister, J.M. Plitzko, TOM software toolbox: acquisition and analysis for electron tomography, J. Struct. Biol. 149 (2005) 227–234.
[26] T. Hrabe, F. Beck, S. Nickell, Automated particle picking based on correlation Peak shape analysis and Iterative classification, Int. J. Med. Biol. Sci. 6 (2012) 1–7.
[27] S.H. Scheres, R. Nunez-Ramirez, C.O. Sorzano, J.M. Carazo, R. Marabini, Image processing for electron microscopy single-particle analysis using XMIPP, Nat. Protoc. 3 (2008) 977–990.
[28] G.R. Pathare, I. Nagy, S. Bohn, P. Unverdorben, A. Hubert, R. Korner, S. Nickell, K. Lasker, A. Sali, T. Tamura, T. Nishioka, F. Forster, W. Baumeister, A. Bracher, The proteasomal subunit Rpn6 is a molecular clamp holding the core and regulatory subcomplexes together, Proc. Natl. Acad. Sci. USA 109 (2012) 149–154.
[29] K.S. Gajiwala, S.K. Burley, Winged helix proteins, Curr. Opin. Struct. Biol. 10 (2000) 110–116.
[30] A. Kao, A. Randall, Y. Yang, V.R. Patel, W. Kandur, S. Guan, S.D. Rychnovsky, P. Baldi, L. Huang, Mapping the structural topology of the yeast 19S proteasomal regulatory particle using chemical cross-linking and probabilistic modeling, Mol. Cell. Proteomics 11 (2012) 1566–1577.
[31] A. Leitner, T. Walzthoeni, A. Kahraman, F. Herzog, O. Rinner, M. Beck, R. Aebersold, Probing native protein structures by chemical cross-linking, mass spectrometry and bioinformatics, Mol. Cell. Proteomics 9 (2010) 1634–1649.
[32] S.J. Wei, J.G. Williams, H. Dang, T.A. Darden, B.L. Betz, M.M. Humble, F.M. Chang, C.S. Trempus, K. Johnson, R.E. Cannon, R.W. Tennant, Identification of a specific motif of the DSS1 protein required for proteasome interaction and p53 protein degradation, J. Mol. Biol. 383 (2008) 693–712.
[33] M.B. Faza, S. Kemmler, V.G. Panse, Sem1: a versatile "molecular glue"?, Nucleus 1 (2010) 12–17
[34] A.S. Konagurthu, J.C. Whisstock, P.J. Stuckey, A.M. Lesk, MUSTANG: a multiple structural alignment algorithm, Proteins 64 (2006) 559–574.